Bistable Defect Structures In Blue Phase Devices

A. Tiribocchi,[1] G. Gonnella,[1] D. Marenduzzo,[2] E. Orlandini,[3] and F. Salvadore[4]

[1]*Dipartimento di Fisica and Sezione INFN di Bari, Università di Bari, 70126 Bari, Italy*
[2]*SUPA, School of Physics, University of Edinburgh, Edinburgh EH9 3JZ, United Kingdom*
[3]*Dipartimento di Fisica and Sezione INFN di Padova, Università di Padova, 35131 Padova, Italy*
[4]*Caspur, via dei Tizii 6/b, 00185 Roma, Italy*

(Received 30 June 2011; published 1 December 2011)

Blue phases are liquid crystals made up by networks of defects, or disclination lines. While existing phase diagrams show a striking variety of competing metastable topologies for these networks, very little is known as to how to kinetically reach a target structure, or how to switch from one to the other, which is of paramount importance for devices. We theoretically identify two confined blue phase I systems in which by applying an appropriate series of electric field it is possible to select one of two bistable defect patterns. Our results may be used to realize new generation and fast switching energy-saving bistable devices in ultrathin surface treated blue phase I wafers.

DOI: 10.1103/PhysRevLett.107.237803 PACS numbers: 61.30.Mp, 42.79.Kr, 61.30.Jf

Liquid crystals are materials with spontaneously broken symmetry; as such they support topological defects of various kinds and may be used as testing grounds for theories on many areas of physics, e.g., the dynamics of cosmic strings and of vortex lines in superfluids and superconductors [1]. Blue phases (BPs) are a spectacular example of soft matter in which a network of such defects self-assembles as a fully periodic cubic three-dimensional structure whose local director has a double-twist configuration [2]. The defects are arranged in a regular fashion, with periodicity at length scales comparable with the wavelength of light. This is the reason why BPs exhibit selective Bragg reflection in the range of visible light and can have interesting applications in fast light modulators [3] and tunable photonic crystals [4]. BPs were initially observed to be stable only in a narrow range of temperature $\sim$1 K, but recently new compounds, stable in a wider interval over $\sim$60 K (including room temperature), have been developed [5,6]. These studies can be considered with good reason as seeds for the recent fabrication of the first blue phase display device with fast switching times [7]. On the other hand, BPs have attracted broader interest among physicists because double-twist cylinders represent a striking example of the so-called Skyrmions, topological excitations encountered in nuclear physics [8], in spinor Bose-Einstein condensates [9], and in ferromagnetic materials, where they have been observed [10].

Theory and experiments have mapped out a number of phase diagrams reporting a remarkably varied range of competing metastable disclination networks [2,11]. However, there are only very few theoretical studies to date regarding the dynamics of the formation of BPs, and virtually none address how to switch from one state to another reversibly in a controlled way. Here we provide the first theoretical study to achieve this goal and give two specific examples of a bistable blue phase I (BPI) system, where an electric field along the appropriate direction can select one of two metastable arrangement of defects. Besides being of interest *per se*, as an intriguing example of controlled defect dynamics, our discovery suggests specific novel geometries which may be used to realize bistable BP-based devices. Devices like the ones we have found are important technologically as each of the bistable states is metastable and is retained after the field is switched off: this fact eliminates the need of having a constant electric field to keep the system in the ''on'' state, hence sharply reducing energy consumption. Some examples of such systems are the zenithal bistable device (ZBD) [12] and surface-stabilized cholesteric texture (SSCT) devices [13]. In the ZBD case bistability relies on flexoelectricity and requires a periodic grating of the surfaces, whereas in the SSCT case it exploits the existence of focal conic defects, which compete against the defect-free helical texture when strong anchoring is used. Several other nematic multistable devices also exist (see, e.g., [14]). Our case is different because the switching occurs between two disclination networks. BP devices such as the one we suggest should also share the faster switching times made possible by BP cells. At the same time, simulations are key to clarify the dynamics of the defect reorganization underpinning bistability [12,14].

In this work we propose two novel BPI (blue phase with O_8^- symmetry) geometries, for which it is possible to design a simple switching on-off schedule that leads to a bistable defect network. In both cases, bistability is present for a sizable range of parameters (quantified below) and is characterized by the presence of two states, which are both metastable when the field is off and have a fully 3D defect structure. The first device we propose relies on surface memory effects which retain the BPI structure on the boundaries, and the two competing states are the standard bulk BPI network and another arrangement, which is only

slightly higher in free energy. The second device exploits the additional frustration driven by strong homeotropic anchoring in a confined thin sample, which conflicts with the bulk ordering. We find that this leads to the appearance of multiple defect states, similar to the ones observed in [15(a)], which, importantly, can be uniquely selected by the application of an electric field along an appropriate direction. Our devices are entirely different from the BP bistable device described in [16]. Firstly, in that device the dielectric anisotropy is negative, while in our case it is positive. Secondly, the switching in [16] is between two field-induced metastable states, which are selected by different values of an applied voltage, whereas in our case the electric field is switched on and off along different directions.

The physics of a BP device may be described by a Landau–de Gennes free energy written in terms of the tensor order parameter $Q_{\alpha\beta}$ [2]. This comprises a bulk term $f_b = \frac{A_0}{2}(1-\frac{\gamma}{3})Q_{\alpha\beta}^2 - \frac{A_0\gamma}{3}Q_{\alpha\beta}Q_{\beta\gamma}Q_{\gamma\alpha} + \frac{A_0\gamma}{4}(Q_{\alpha\beta}^2)^2$ and a distortion term [2] $f_d = \frac{K}{2}(\partial_\beta Q_{\alpha\beta})^2 + \frac{K}{2}\times(\epsilon_{\alpha\zeta\delta}\partial_\zeta Q_{\delta\beta} + 2q_0 Q_{\alpha\beta})^2$, where K is the elastic constant and the pitch of the cholesteric liquid crystal is given by $p \equiv 2\pi/q_0$. A_0 is a constant, γ controls the magnitude of the ordering, and $\epsilon_{\alpha\zeta\delta}$ is the Levi-Civita antisymmetric third-rank tensor. The constants A_0, K, and γ are chosen in order to be in the appropriate region of the phase diagram [11]. We have set $A_0 = 0.0034$, $K = 0.005$, $\gamma = 3.775$ for which BPI is stable. This choice may be mapped to a rotational viscosity equal to 1 P, (Frank) elastic constants equal to $\sim$30 pN, and a blue phase periodicity equal to 300 nm. Moreover, one space and time unit correspond to 0.0125 μm and 0.0013 μs. The contribution of the boundaries is encoded in a surface free-energy term, given by $f_s = 1/2W_0(Q_{\alpha\beta} - Q_{\alpha\beta}^0)^2$, where W_0 (larger than 0.01 N/m in our simulations) controls the anchoring strength and $Q_{\alpha\beta}^0$ is the order parameter at the surfaces. The interaction with an external electric field $\mathbf{E}$ is accounted for by an additional term, $-\frac{\varepsilon_a}{12\pi}E_\alpha Q_{\alpha\beta}E_\beta$, where ε_a (here taken >0) is the dielectric anisotropy of the material. The electric field may be quantified via the dimensionless number $e^2 = 27\varepsilon_a E_\alpha^2/(32\pi A_0\gamma)$. By assuming a dielectric anisotropy of $\sim$100 [17], one finds that an electric field of 1–10 V/μm corresponds to $e^2 \sim$ 0.003–0.3. The simulation domains along the three coordinate axes are L_x, L_y, and L_z, respectively, with periodic boundaries along $\hat{x}$ and $\hat{y}$. All of our results are performed on lattices of dimensions $32\times32\times32$. The equation of motion for $\mathbf{Q}$ is $D_t\mathbf{Q} = \Gamma\mathbf{H}$, where Γ is a collective rotational diffusion constant and D_t is the material derivative for rodlike molecules [18]. The molecular field $\mathbf{H}$ is the thermodynamic force that drives the system towards the equilibrium [18]. The velocity field obeys a Navier-Stokes equation with a stress tensor generalized to describe LC hydrodynamics [18]. The interplay between the velocity field and the order parameter is referred to as backflow. To solve the equations of motion, we used a hybrid lattice Boltzmann algorithm, as in [14].

The usual zero-field defect structure in the BPI cell is shown in Fig. 1(a). We first focus on the case in which the director field is fixed at the top ($z = L$, L being the sample size) and bottom ($z = 0$) boundaries of the cubic cell to its stable structure in the absence of a field. This may be achieved by pinning due to impurities or through surface memory effects [19]. Figures 2(a)–2(d) show the evolution of the defect network in response to an electric field switched on and off first along $\hat{x}$, then along $\hat{y}$. During the cycle the defect dynamics is highly nontrivial and is characterized by a complex reorganization driven by the electric field, and depending on its direction. In particular, after the application of the field along $\hat{x}$, the defects twist and bend and eventually recombine, annihilating in the bulk and forming defect arcs pinned at the walls ($t_1 - t_4$). The voltage ($\Delta V_y = E_y L_y$) is chosen strong enough to break the defect structure in the bulk. When the field is switched off, some disclinations migrate back to the center of the cell, giving rise to connected boundary arcs that span the entire device ($t_5 - t_8$). The system gets stuck into a stationary metastable state (t_8), whose free energy is different from the one of the zero-field state (see inset of Fig. 2, top panel). Because of the anisotropy of the BPs, it is now interesting to ask what is the defect dynamics if the electric field acts on a different direction. Starting from the configuration at time t_8, we have switched on an electric field along the $\hat{y}$ direction, with voltage equal to the one chosen for the field in the $\hat{x}$ direction. The defects now start to deform, bending in the direction of the field (t_9), and then move towards the bulk where they met and form unstable branching points that annihilate. This second field-induced state (t_{12}) is again (as the one at time t_4) characterized by boundary arcs. By switching off the field, the system reorganizes as the boundaries force the disclinations towards the bulk: surprisingly, the dynamics now leads back to the starting bulk BPI [Fig. 1(a)]. Bistability is affected by the voltages used in the switching. We have simulated the same device for $e^2 \sim 0.2, 0.3$ and found that it is bistable in both cases. On the other hand, bistability is lost for $e^2 < 0.2$ and the switching dynamics is now characterized by a reversible cycle in which a zero-field state

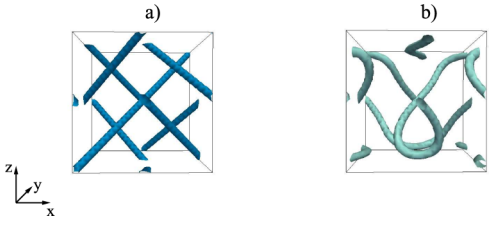

FIG. 1 (color online). Equilibrium disclination networks for BPI when (a) the structure is strongly anchored at both walls and when (b) there is homeotropic anchoring at both walls.

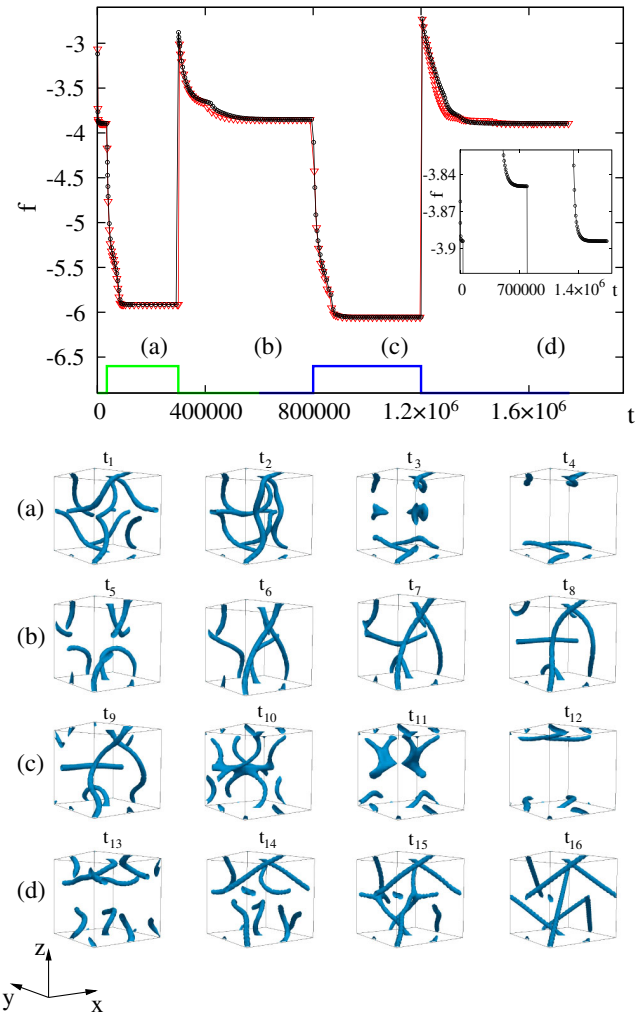

FIG. 2 (color online). Free-energy evolution (top panel) of the BPI device with FBCs, with (triangles) and without (circles) backflow. Parameters were $A_0 = 0.0034$, $K = 0.005$, $\gamma = 3.775$, $e^2 \sim 0.2$ (corresponding to a field of ~ 8 V/μm). The evolution of the defects under an applied field is reported in the bottom panel. The step function in the top panel is $\neq 0$ when the field is on. From $t = 0$ up to $t = 35\,000$ the system relaxes to the stable BPI configuration in Fig. 1(a). An electric field along $\hat{x}$ is switched on at $t = 35 \times 10^3$ and the equilibrium field-induced state is reached at $t_4 = 30 \times 10^4$. The corresponding free energy is shown in (a), top panel. Then the field is switched off and the system relaxes to a new metastable state ($t_8 = 80 \times 10^4$) [(b) in the bottom panel] characterized by a new free energy, slightly higher than the bulk BPI value. An electric field along $\hat{y}$ is then switched on and off at $t_{12} = 120 \times 10^4$ [(c) and (d) in the top panel]. Strikingly, the relaxation process brings the system back to the equilibrium state without field.

[different from the bulk BPI structure, Fig. 1(a)], obtained after the application of the electric field along $\hat{x}$, is recovered even after switching along $\hat{y}$. Note also that the results in Fig. 2 refer to BP devices with $\varepsilon_a > 0$: intriguingly, in the case of negative dielectric constant the device can never get back to the bulk BPI state. This may be due to the fact that in the presence of a field the director can form a helix along the field, and this is not different enough in free energy from the BP state to drive a reorganization of the unit cell once the field is removed. To check the robustness of our results, we have also simulated the device with different values of A_0 and γ (e.g., $A_0 = 0.0012$ and $\gamma = 5.085$), again leading to a stable BPI—even in this different region of phase space we find that the device is bistable. Finally, in Fig. 2, top panel, we also compare the free energies as a function of time both in the presence and the absence of hydrodynamics. The effect of backflow is to slightly speed up all relaxations, without deep consequences on the dynamic evolution.

We now turn to the case of different boundary conditions. Fixed boundary conditions (FBCs), such as the ones we have just employed, have often been used in cholesterics and BPs [19]. However, in practice it is more feasible to control the alignment of the director field at the boundaries by chemical treatment or rubbing. The former technique typically is used to enforce homeotropic (or perpendicular) anchoring of the director at the wall, the latter yields homogeneous (or parallel) anchoring. Therefore, it is interesting to know how these boundaries affect the switching dynamics of a BP device, and, importantly, whether they can still lead to a bistable behavior. In what follows we focus on a BPI device with *homeotropic* anchoring at both walls. To the best of our knowledge there is only one study about the equilibrium disclination configuration in confined BPI cell with homeotropic anchoring [15(a)] while nothing is known about electric field effects in these thin cells. As we shall see, by using the same electric field dynamical schedule adopted for the cell with FBCs, it is still possible to realize a switchable bistable device, albeit with some key conceptual differences with respect to the device in Fig. 1(a). The first one is that homeotropic anchoring affects the zero-field equilibrium defect structure [Fig. 1(b)], now characterized by bent disclinations depinned from the walls—the original topology of BPI being preserved. The second important difference is that the change of the boundary conditions affects the dynamic evolution under an electric field: the minimum value required to destabilize the initial topology is now $e^2 \sim 0.05$. This decrease in the threshold is because the wall now pins the zero-field structure more weakly than in the case of Fig. 1. In spite of these differences, there is a range in which the device shows bistability, and the switching dynamics of the defect network is reported in Fig. 3. When the electric field is switched on along the $\hat{x}$ direction ($t_1 - t_4$), the defects start to deform, bend, and form a spectacular double-helix pattern in the bulk, accompanied by columnar defects at the wall. This structure is induced and stabilized by the electric field, yet it only suffers minor rearrangements as the field is switched off. This double-helical state has already been observed in Ref. [15(a)] in the *absence* of a field—it could be selected for instance by

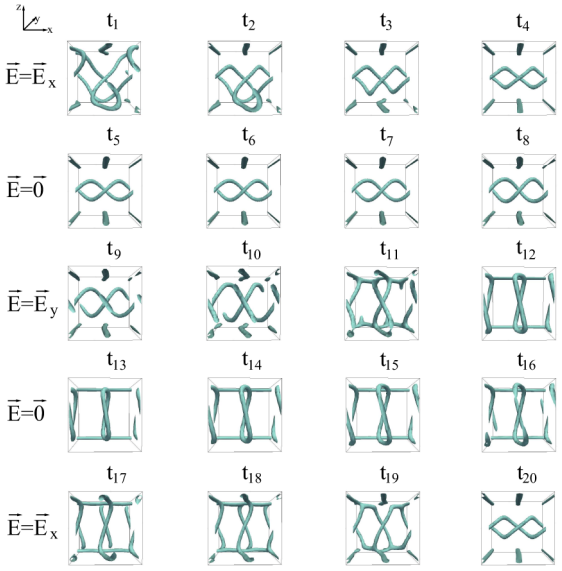

FIG. 3 (color online). Defect evolution with homeotropic anchoring under an applied electric field. Parameters are the same as in Fig. 2. The electric field (~ 4.5 V/μm, i.e., with $e^2 \sim 0.06$) is switched on along $\hat{x}$ at time $t = 10 \times 10^4$ [Fig. 1(b) for the steady state] and the evolution dynamics is reported in the first row. A steady state double-helix defect is attained at time $t_4 = 98.7 \times 10^4$. When the field is switched off the defect structure is almost unaltered (steady state reached at time $t_8 = 117.7 \times 10^4$). Then field (~ 4 V/μm, i.e., with $e^2 \sim 0.05$) is switched on along $\hat{y}$. The double-helix disclination transforms into a steady state with twisted ring defects ($t_{12} = 155.6 \times 10^4$) stable after switching off ($t_{16} = 194.2 \times 10^4$). Bistability requires a route back to the double-helix state: this is provided by a further application of a field along $\hat{x}$ (steady state at $t_{20} = 223.4 \times 10^4$).

tuning the device thickness. When we switch on the field again, now along the $\hat{y}$ direction (see snapshots $t_9 - t_{16}$), the bent double-helix moves towards the walls ($t_9 - t_{10}$) where it joins up with the columnar disclinations to form a transient interconnected structure (t_{11}) which later on relaxes to an array of twisted ring defects in the bulk, accompanied again by straight disclinations, this time at right angles with the one associated with the double-helical state (t_{12}). Once more the field-induced rings do not change much upon switching off ($t_{12} - t_{16}$). We note that a state similar to these ring defects has recently been observed in Ref. [15(b)], however, in a system with *homogeneous* anchoring at the walls. Our simulations therefore show that the number of possible defect networks in these thin BP cells are even more than previously thought. In order to behave as a switchable bistable device, our system still needs to be able to reconstruct the double-helical state starting from the ring defect structure. This is indeed what happens if the field is switched on and off along the $\hat{x}$ direction (as in the first cycle). The ring defects initially enlarge and touch the walls where disclination lines reform ($t_{17} - t_{18}$). Thereafter the double-helix pattern reconstructs in the bulk (t_{19}) and later on stabilizes. Thus our thin BP sample with homeotropic anchoring behaves as a bistable device, and the two switchable states are the double-helical and twisted ring structures—unlike the surface memory device, none of these equals the zero-field stable state.

In summary, we have investigated the hydrodynamics of a cubic BPI cell and proposed two systems, differing in the boundary conditions, which can switch between two bistable disclination structures under the action of an applied field. In the first one we have fixed boundary conditions at both walls, while in the second one we considered homeotropic anchoring. In the FBCs cell, the two switchable states are the zero-field BPI and another metastable defect network. The device with homeotropic anchoring, on the other hand, switches between two states which are metastable in the absence of a field. In one of these states the defects form a double helix, whereas in the other one they arrange as an array of twisted rings—these configurations are alternatively observed by varying the direction and the magnitude of the electric field. The bistable behavior of this device is promising for technological applications to energy-saving devices because, in principle, the required anchoring could easily be achieved. The physical reason behind the viability of BP bistable devices may be the glassy free-energy profile which admits a number of competing metastable minima, each of which is potentially suited for their design, provided a suitable kinetic route to achieve reversible switching is discovered. In this respect, one may expect that even more BP bistable systems may be found in the future.

[1] M. B. Hindmarsh and T. W. B. Kibble, Rep. Prog. Phys. **58**, 477 (1995); A. Bulgac *et al.*, Science **332**, 1288 (2011); R. A. Borzi *et al.*, Science **315**, 214 (2007).
[2] D. C. Wright and N. D. Mermin, Rev. Mod. Phys. **61**, 385 (1989), and references therein.
[3] V. E. Dmitrenko, Liq. Cryst. **5**, 847 (1989).
[4] P. Etchegoin, Phys. Rev. E **62**, 1435 (2000).
[5] H. Kikuchi *et al.*, Nature Mater. **1**, 64 (2002).
[6] H. J. Coles and M. N. Pivnenko, Nature (London) **436**, 997 (2005).
[7] www.physorg.com/news129997960.html.
[8] G. E. Brown and M. Rho, Phys. Rep. **363**, 85 (2002).
[9] U. Al Khawaja and H. Stoof, Nature (London) **411**, 918 (2001).
[10] S. Mühlbauer *et al.*, Science **323**, 915 (2009).
[11] A. Dupuis, D. Marenduzzo, and J. M. Yeomans, Phys. Rev. E **71**, 011703 (2005).
[12] C. Denniston and J. M. Yeomans, Phys. Rev. Lett. **87**, 275505 (2001); L. A. Parry-Jones and S. J. Elston, J. Appl. Phys. **97**, 093515 (2005).
[13] D. K. Yang *et al.*, Annu. Rev. Mater. Sci. **27**, 117 (1997); J. Appl. Phys. **76**, 1331 (1994).
[14] R. Barberi, M. Giocondo, and G. Durand, Appl. Phys. Lett. **60**, 1085 (1992); J. Kim, M. Yoneya, and H.

Yokoyama, Nature (London) **420**, 159 (2002); A. Tiribocchi *et al.*, Appl. Phys. Lett. **97**, 143505 (2010).
[15] (a) J. I. Fukuda and S. Zumer, Phys. Rev. Lett. **104**, 017801 (2010); (b) **106**, 097801 (2011).
[16] C.-T. Wang *et al.*, Appl. Phys. Lett. **96**, 041106 (2010).
[17] L. Rao *et al.*, Appl. Phys. Lett. **98**, 081109 (2011).
[18] A. N. Beris and B. J. Edwards, *Thermodynamics of Flowing Systems* (Oxford University Press, Oxford, 1994).
[19] T. C. Lubenski, Phys. Rev. A **6**, 452 (1972); A. Tiribocchi *et al.*, Soft Matter **7**, 3295 (2011).